

Tracing the Evolution of Angucyclinone Monooxygenases: Structural Determinants for C-12b Hydroxylation and Substrate Inhibition in PgaE

Pauli Kallio,[†] Pekka Patrikainen,[†] Georgiy A. Belogurov,[†] Pekka Mäntsälä,[†] Keqian Yang,[‡] Jarmo Niemi,[†] and Mikko Metsä-Ketelä^{*,†}

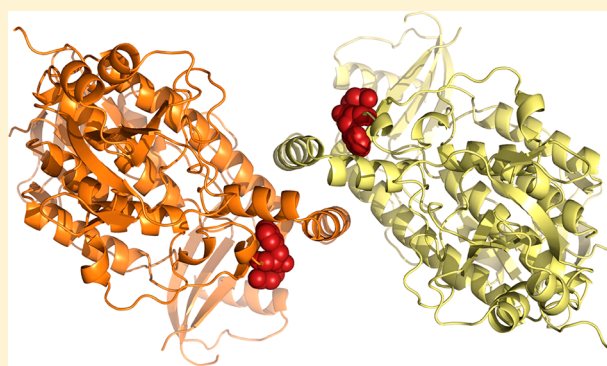
[†]Department of Biochemistry and Food Chemistry, University of Turku, FIN-20014 Turku, Finland

[‡]State Key Laboratory of Microbial Resources, Institute of Microbiology, Chinese Academy of Sciences, Beijing 100101, PR China

S Supporting Information

ABSTRACT: Two functionally distinct homologous flavoprotein hydroxylases, PgaE and JadH, have been identified as branching points in the biosynthesis of the polyketide antibiotics gaudimycin C and jadomycin A, respectively. These evolutionarily related enzymes are both bifunctional and able to catalyze the same initial reaction, C-12 hydroxylation of the common angucyclinone intermediate prejadomycin. The enzymes diverge in their secondary activities, which include hydroxylation at C-12b by PgaE and dehydration at C-4a/C-12b by JadH. A further difference is that the C-12 hydroxylation is subject to substrate inhibition only in PgaE. Here we have identified regions associated with the C-12b hydroxylation in PgaE by extensive chimeragenesis, focusing on regions surrounding the active site.

The results highlight the importance of a hairpin- β motif near the dimer interface, with two nonconserved residues, P78 and I79 (corresponding to Q89 and F90, respectively, in JadH), and invariant residue H73 playing key roles. Kinetic characterization of PgaE variants demonstrates that the secondary C-12b hydroxylation and substrate inhibition by prejadomycin are likely to be interlinked. The crystal structure of the PgaE P78Q/I79F variant at 2.4 Å resolution confirms that the changes do not alter the conformation of the β -strand secondary structure and that the side chains of these residues in effect point away from the active site toward the dimer interface. The results support a catalytic model for PgaE containing two binding modes for C-12 and C-12b hydroxylations, where binding of prejadomycin in the orientation for C-12b hydroxylation leads to substrate inhibition. The presence of an allosteric network is evident based on enzyme kinetics.



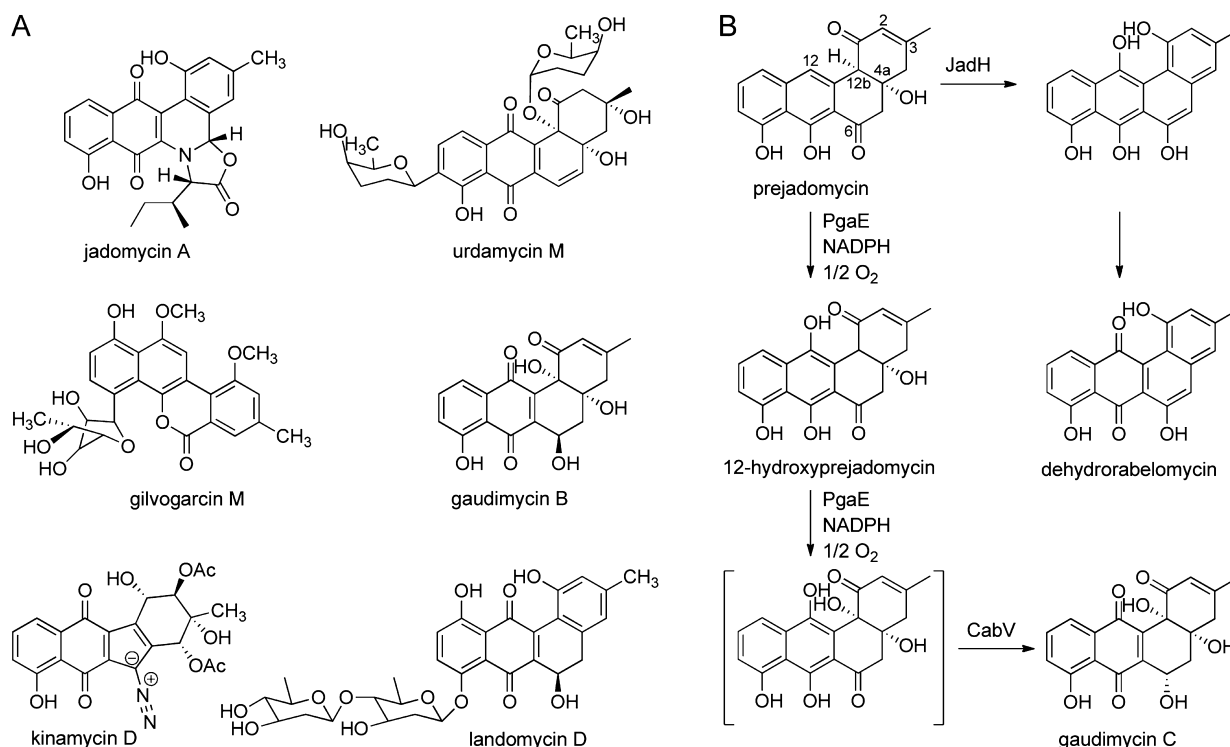
Bacteria of the genus *Streptomyces* are known as valuable producers of natural products, many of which have found applications in medicine and agriculture.¹ These compounds are produced through secondary metabolic pathways that are renowned for their natural diversity; sequencing projects have revealed that >30 such pathways may be encoded in the genome of a single *Streptomyces* species with a high degree of strain to strain variation.² One distinct group of bacterial secondary metabolites consists of the angucyclines, which are aromatic polyketides rich in biological activities and chemical scaffolds (Scheme 1A). Many of these compounds are especially potent anticancer agents with diverse activities against numerous cellular targets. For instance, jadomycins have been identified as Aurora kinase inhibitors,³ kinamycins inhibit the decatenation activity of DNA topoisomerase II,⁴ while gilvocarcins harbor a unique mode of action involving photoactivated [2+2] cycloaddition with DNA.⁵ The more recently discovered landomycins induce apoptosis through a yet unknown mechanism and are active against multidrug resistant cells.⁶

The diversity of natural products isolated from *Streptomyces* may be explained, at least in part, by selective pressure favoring chemical polymorphism over preservation of specific biosynthetic functions. Because by definition gene products involved in secondary metabolism are not directly essential to the survival of the host, latent promiscuous enzymatic activities are relatively free to evolve further. This is sometimes manifested as unexpected changes in catalytic specificities of individual biosynthetic proteins during enzyme evolution,⁷ which may have a dramatic impact on the outcome of a given secondary metabolite pathway. Examples of enzymes that have drastically diverged from their ancestral counterparts include RdmB from the rhodomycin pathway, which is homologous to classical methyl transferases but explicitly functions as a C-10 hydroxylase;⁸ SnoaL2 from the nogalamycin pathway, which is involved in C-1 hydroxylation⁹ even though the protein is similar

Received: March 25, 2013

Revised: May 31, 2013

Published: June 3, 2013

Scheme 1. Angucycline Antibiotics and Early Tailoring Steps in Their Biosynthesis^a


^a(A) Structures of the modified angucyclines jadomycin A, gilvocarcin M, and kinamycin D and the benz[*a*]anthracene metabolites urdamycin M, gaudimycin B, and landomycin D. (B) Tailoring reactions catalyzed by the two related flavoenzymes JadH and PgaE investigated in this study. On the gaudimycin pathway, the C-12b hydroxylation by PgaE is followed by C-6 ketoreduction through the action of CabV, an enzyme of the short chain alcohol dehydrogenase/reductase superfamily, to produce gaudimycin C.¹³

to polyketide cyclases in structure and sequence;^{10,11} and the flavoprotein monooxygenase JadH involved in jadomycin biosynthesis, which additionally catalyzes an atypical secondary dehydration reaction.^{12,13} A detailed understanding of these changes in enzyme function and substrate specificity during the evolution of the biosynthetic pathways may hold a key for structure-based protein design for the synthesis of novel natural products with improved biological activities.

The biosynthesis of the carbon skeletons of angucyclines proceeds through canonical pathways that have been well established for type II polyketides.^{14,15} The assembly is initiated via iterative Claisen condensations of acetyl- and malonyl-coenzyme A units in a manner reminiscent to the biosynthesis of fatty acids in bacteria. However, the polyketide synthases responsible for the assembly do not reduce the elongating carbon chain during synthesis, and subsequently, a long polyketide is formed. During these initial steps, the highly reactive polyketide is tethered to an acyl carrier protein, and the first stable intermediate of many pathways, prejadomycin (also known as 2,3-dehydro-UWM6), is released only after controlled reduction and cyclization.^{14,16,17}

The great diversity of angucyclines is generated in tailoring reactions, which modify the formed polyketide aglycone. Many angucycline metabolites (e.g., the urdamycins, gaudimycins, and landomycins) are built around a benz[*a*]anthracene carbon frame, while several others (e.g., the jadomycins, kinamycins, and gilvocarcins) are further modified in oxidative rearrangement processes (Scheme 1A). Recent studies have uncovered the fact that the key branching point in the biosynthesis of these two classes of angucyclines is the action of homologous bifunctional NADPH-dependent flavoprotein hydroxylases. On all of the

pathways, the corresponding enzymes share the same initial activity, the NADPH- and O₂-dependent hydroxylation of prejadomycin at C-12,^{12,13,18,19} but the proteins differ with respect to their subsequent catalytic reactions: the enzymes from pathways leading to benz[*a*]anthracenes (UrdE,¹³ urdamycin; PgaE¹⁸ and CabE,¹³ gaudimycin; LanE,¹³ landomycin) are able to catalyze a second oxygen-dependent hydroxylation at position C-12b, whereas the other related enzymes (GilOI,¹⁹ gilvocarcin; JadH,¹² jadomycin; AlpG, kinamycin) are responsible for dehydration at C-4a/C-12b, resulting in the formation of dehydrorabelomycin (Scheme 1B). The activities of these enzymes have been confirmed *in vitro*, with the exception of those of AlpG, for which the evidence stems from phylogenetic analysis²⁰ and from the observation that the biosynthesis of the benzo[*b*]fluorene chromophore of kinamycins proceeds via dehydrorabelomycin.²¹ Another profound difference is seen in the kinetic behavior with respect to prejadomycin utilization in some of these enzymes. While the C-12 hydroxylation reaction catalyzed by PgaE is modulated by substrate inhibition, the JadH reaction follows typical Michaelis–Menten saturation kinetics.^{12,18} In the case of PgaE, the reaction is characterized by an unusual temporal separation of the two reaction phases, where C-12b hydroxylation is not initiated prior to depletion of prejadomycin.¹⁸

The structure determination of PgaE²² confirmed the similarity of the enzyme to related aromatic hydroxylases such as the much studied *p*-hydroxybenzoate hydroxylase (pHbH) from *Pseudomonas fluorescens*^{23,24} and indicated that the enzyme is a dimer in solution and in the crystal. The protein consists of three domains, the FAD-binding domain, the middle domain, and the C-terminal domain (Figure 1A).²² The Rossmann-type

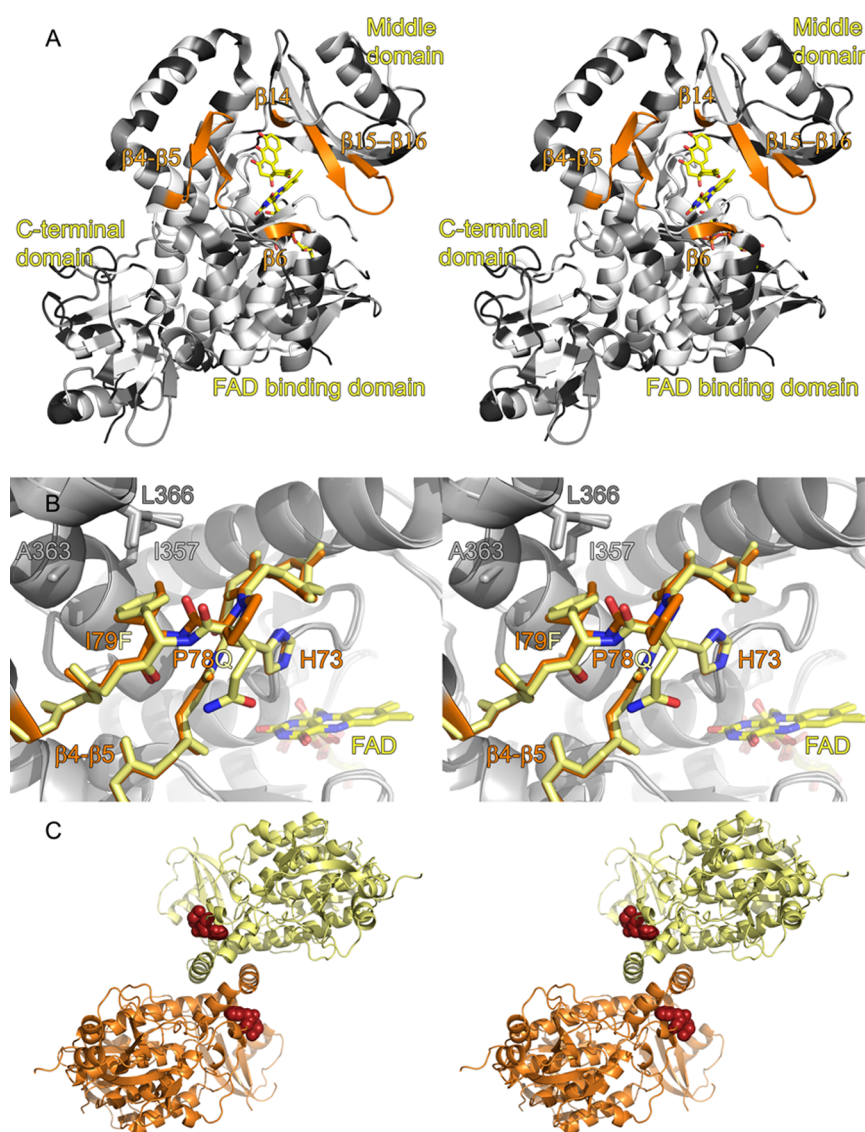


Figure 1. Crystal structure of native PgaE and the P78Q/I79F variant described in this study. (A) Overall structure of PgaE with prejadomycin docked into the active site and regions of interest highlighted. The protein has been color-coded on the basis of its similarity with JadH in the following manner: black for dissimilar amino acid residues, gray for similar residues, white for identical residues, and orange for the region of interest. (B) Comparison of native (orange) and P78Q/I79F (yellow) variant structures of PgaE around the $\beta 4$ – $\beta 5$ hairpin. (C) Dimer structure of the PgaE P78Q/I79F variant with the mutated residues highlighted as red space-filling models.

FAD-binding domain forms the core of the protein that is responsible for binding of the cofactor, while the middle domain has been suggested to shape the roof of the substrate binding pocket. The function of the C-terminal domain remains unknown, and although the fold of the domain resembles thioredoxin, it lacks the two conserved catalytic cysteine residues. Structural and mechanistic studies of pHBH have uncovered a multistep reaction sequence, which involves extensive conformational changes and movement of both the FAD and the protein during the reaction cycle.^{25,26} In the case of PgaE, the binary complex of the enzyme crystallized with FAD in the “in” and the protein in the “open” conformation, which has been proposed to represent the conformation that is ready for substrate binding or product release.²⁷

The aim of this study was to identify the specific structural determinants for the characteristic functional features of PgaE versus JadH (58% amino acid sequence identity). The initial step was to use the available crystal structures of PgaE and CabE²² and

the amino acid sequences of the orthologous hydroxylases UrdE and LanE for comparison with the amino acid sequence of JadH, GilOI, and AlpG to find the active site regions that could be affiliated with the catalytic differences. The approach was then to modify the selected regions in PgaE by an overlap extension polymerase chain reaction (PCR) chimeragenesis approach to correspond to the JadH template and to monitor the effect on C-12b hydroxylation, substrate inhibition, and C-4a/C-12b dehydration of the substrate prejadomycin.

■ EXPERIMENTAL PROCEDURES

Mutagenesis. Targeted mutagenesis of *pgaE* was conducted using a modified four-primer overhang extension PCR method.²⁸ In the first-round PCR, the target gene was amplified in two fragments, which contained overlapping mutagenesis primers (Table S1 of the Supporting Information) complementary to the *jadH* template at the site of chimeragenesis that were used in combination with outer primers 5′-GTAACAAAGCGGAC-

AAAGC-3' (forward) and 5'-tataagcttTCAGCCGGTGAGCG-GTGC-3' (reverse). The template was either pBHBA-pgaE²² or, when preparing multichimeric genes, one of the derived variant constructs. In the second-round PCR, the primary amplification products were mixed together (serving as template) with the outer primers to produce the final full-length mutated *pgaE*. The product was then extracted, subcloned into pBHBA²⁹ as a BglII/HindIII fragment, and confirmed by sequencing (Eurofins MWG Operon).

Overexpression and Purification of the Enzymes. The PgaE variants were overexpressed using construct pBHBA as N-terminally His-tagged fusion proteins in *Escherichia coli* strain TOP10. The main cultures (250 mL of 2× YT medium with ampicillin) were inoculated using a 1:100 volume of overnight precultures and grown at 30 °C and 250 rpm until they were induced with 0.02% L-arabinose at an A_{600} of 0.5, followed by incubation at room temperature at 100–150 rpm for 18 h. The cells were harvested by centrifugation and washed twice with cold 1× PBS buffer, pelleted, and stored at –20 °C. Cell lysis was conducted using a French press (20 mL of buffer A with 0.1 mg of DNase II); Triton X-100 (1%) was added to the lysate, and the debris was removed by centrifugation (18000 rpm for 1 h). Purification was conducted in a single step with TALON His-tag purification cobalt affinity resin (Clontech) according to the manufacturer's instructions. The proteins were loaded in buffer A [20 mM Na₃PO₄, 100 mM NaCl, 10% glycerol, and 5 mM imidazole (pH 7.5)] and eluted in buffer B (buffer A but with 250 mM imidazole). The elution fractions were stored at –20 °C after addition of glycerol to a final concentration of 50% (v/v). The purity of the enzymes was estimated to be >95% based on sodium dodecyl sulfate–polyacrylamide gel electrophoresis (SDS–PAGE) analysis (Figure S1 of the Supporting Information), and the concentration was estimated using the Bradford dye binding method.³⁰

Enzyme Activity Characterization. The default enzyme reaction mixtures contained 30 μM prejadomycin supplied in methanol [6% (v/v)] and 100 μM NADPH in 100 mM potassium phosphate buffer (pH 7.6) in a final volume of 250 μL. The enzyme concentrations were adjusted to achieve complete conversion of prejadomycin in 10–15 min. The kinetic measurements were taken with 78.5 nM (C-12 hydroxylation) and 19.6 nM (C-12b hydroxylation) native PgaE, 76.7 and 383.4 nM PgaE β4–β5, 50.6 and 16.8 nM PgaE β4, 40.2 and 302.2 nM PgaE β5, 23.7 and 355.2 nM PgaE P78Q/I79F, 48.9 and 12.2 nM PgaE P78Q, and 49.6 and 99.2 nM PgaE I79F. The C-12 hydroxylation of PgaE H73A was analyzed at an enzyme concentration of 54.2 nM. The activities were monitored using a MultiskanGO UV–vis microplate spectrophotometer (Thermo Scientific) on 96-well plates by measuring the consumption of prejadomycin at 406 nm in relation to the disappearance of the intermediate at 510 nm.¹⁸ When the C-12b hydroxylation reaction alone was assessed, 12-hydroxyprejadomycin was extracted as described previously¹⁸ and used as a substrate in place of prejadomycin.

The initial reaction rates for the different PgaE variants were measured by monitoring the declining progress curves of the reactions at different substrate concentrations using either prejadomycin (C-12 hydroxylation) or 12-hydroxyprejadomycin (C-12b hydroxylation).¹⁸ The obtained initial rates were plotted versus the concentrations. The interpretation of the data for the C-12 hydroxylation reactions is presented in the text of the Supporting Information. The data for the C-12b hydroxylation reactions were fit using a rate equation describing a sigmoidal

relationship (Figure S2 of the Supporting Information) as described previously.¹⁸ Determination of the initial slopes and the data analysis for C-12b hydroxylation were performed using Origin 8.0 (OriginLab Corp.).

Protein Crystallization, Structure Determination, and Docking Experiments. The P78Q/I79F PgaE variant was crystallized by the hanging-drop method under conditions similar to those used for the native enzyme:²² 7 mg/mL enzyme containing 5 mM NADPH and saturated prejadomycin in methanol [14% (v/v)]. The well solution consisted of 0.1 2-(N-morpholino)ethanesulfonic acid (pH 6.4), 1.8 M ammonium sulfate, and 2% dioxane. The drops yielding crystals contained protein solution and well solution in a 1:1 ratio. The diffraction data obtained at the European Synchrotron Radiation Facility (Grenoble, France) were processed with MOSFLM,³¹ and the data were scaled using SCALA from the CCP4 package.³² The structure was determined by molecular replacement using MOLREP³³ in the CCP4 package using the native structure as a search model, finalized by manual building in COOT³⁴ and refinement using REFMAC.³⁵ Structure validation was conducted with the MolProbity web server.³⁶ Statistics for the data collection and refinement are given in Table S2 of the Supporting Information. The PRODRG server³⁷ was used to prepare a model of prejadomycin. Docking of the ligand was done with GOLD using Discovery Studio (Discovery Studio Modeling Environment, version 3.5, Accelrys Software Inc.). Figure 1 depicting protein structures was prepared using PyMol (The PyMOL Molecular Graphics System, version 1.3, Schrödinger, LLC).

RESULTS

Identification of Regions Involved in Substrate Recognition. Phylogenetic analysis (Figure 2) and structure-

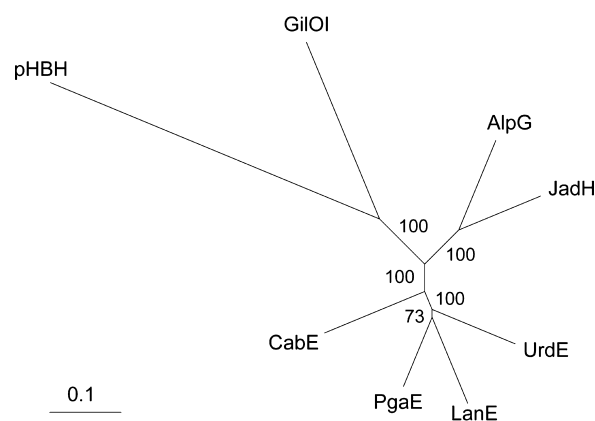


Figure 2. Phylogenetic relationships of the angucycline monooxygenases investigated in this study with the much studied *p*-hydroxybenzoate hydroxylase (pHBH, Protein Data Bank entry 1PDH) shown as an out-group. The tree was constructed by the neighbor-joining method as described previously,²⁰ and bootstrap values for the clades are displayed. The scale bar represents 10% dissimilarity.

based multiple-sequence alignment (Figure S3 of the Supporting Information) demonstrated the evolutionary relationships and high level of sequence similarity, respectively, between PgaE, LanE, CabE, and UrdE and JadH, GilOI, and AlpG. When the crystal structure of PgaE was color-coded on the basis of the JadH template, most of the dissimilar amino acid residues (Figure 1A, black) were found on the surface of the protein, while many of

the similar (gray) and identical (white) amino acids were located in the interior or involved in binding of the cofactor FAD. Surprisingly, the similarity extended to a large degree to the regions lining the proposed binding site cavity, and the main differences could be attributed to four distinct segments (Figure 1A, orange). The most obvious nonconservative substitutions around the putative substrate binding site in PgaE with respect to JadH were in the $\beta 4$ – $\beta 5$ (residues 70–82 of PgaE) and $\beta 6$ (residues 92–94) regions, which are part of the FAD binding domain, and the $\beta 14$ (residues 189 and 190) and $\beta 15$ – $\beta 16$ (residues 201–209) β -strands from the so-called middle domain (Table 1).

Table 1. Sequence Alignment of the Regions Investigated in This Study

Region	Enzyme	Amino acids	
$\beta 4$ – $\beta 5$	PgaE	67	ETS – TQGHFGGLPFDG – VLE 85
	JadH	78	ETS – PMGHFGGVQFDYT – VLE 96
$\beta 4$	PgaE	67	ETS – TQ – GHF 74
	JadH	78	ETS – PM – GHF 85
$\beta 5$	PgaE	74	FGG – LPFDG – VLE 85
	JadH	85	FGG – VQFDYT – VLE 96
$\beta 6$	PgaE	91	A – KTV – PQ 96
	JadH	102	A – RGI – PQ 107
$\beta 14$	PgaE	187	PR – MI – GE 192
	JadH	198	PR – FL – GE 203
$\beta 15$ – $\beta 16$	PgaE	198	MVM – VGPLPGGIT – RII 212
	JadH	211	MVM – AAPLAEGVD – RII 225

Chimeric Proteins with Multiple Changes Alter the C-12b Hydroxylation Activity of PgaE. The most noticeable region of interest was the small hairpin- β motif ($\beta 4$ – $\beta 5$) at the back end of the active site cavity (Figure 1A), which on the basis of docking experiments is in direct contact with the substrate prejadomycin on the opposite side of the ligand from the cofactor FAD. Swapping of the entire $\beta 4$ – $\beta 5$ region according to the JadH template sequence had a dramatic impact on PgaE function, as the second hydroxylation step was significantly impaired. The ability of the $\beta 4$ – $\beta 5$ chimera to convert prejadomycin remained comparable to that of the native enzyme, but it displayed >90% lower relative activity toward the C-12b hydroxylation (Figure 3A,B). To probe the combined effects of the other regions surrounding the substrate binding site, we next extended the chimeragenesis to cover the $\beta 6$, $\beta 14$, and $\beta 15$ – $\beta 16$ secondary structure regions together with the exchanged $\beta 4$ – $\beta 5$ sheets (Figure 1A). While changing the additional $\beta 6$ or $\beta 15$ – $\beta 16$ regions did not have any further effect on the reaction profile (Figure 3C,D), replacing the adjacent $\beta 14$ to generate the PgaE $\beta 4$ – $\beta 5$ / $\beta 14$ double chimera (Figure 3E) surprisingly resulted in the reversal of the activity slightly toward the native profile, where the C-12b hydroxylation appeared to be no longer effectively blocked. Simultaneous incorporation of a third mutated region, $\beta 6$, to produce the $\beta 4$ – $\beta 5$ / $\beta 6$ / $\beta 14$ triple chimera further enhanced the effect, resulting in an activity profile equivalent to that of wild-type PgaE (Figure 3F). The two other triple chimeras, $\beta 4$ – $\beta 5$ / $\beta 6$ / $\beta 15$ – $\beta 16$ and $\beta 4$ – $\beta 5$ / $\beta 14$ / $\beta 15$ – $\beta 16$, remained deficient in their ability to catalyze C-12b hydroxylation (Figure 3G,H). Finally, when all four regions in

PgaE were exchanged with their JadH counterparts, the activity of the $\beta 4$ – $\beta 5$ / $\beta 6$ / $\beta 14$ / $\beta 15$ – $\beta 16$ quadruple chimera (Figure 3I) resembled that of the initial $\beta 4$ – $\beta 5$ chimera.

Further Analysis of the $\beta 4$ – $\beta 5$ Region Reveals Amino Acids That Are Important for C-12b Hydroxylation and Substrate Inhibition. Next, the $\beta 4$ – $\beta 5$ region associated with C-12b hydroxylation was dissected into smaller subregions to identify the amino acid(s) responsible for the observed effect. The mutants generated were then subjected to full kinetic characterization to analyze their ability to catalyze the C-12 and C-12b hydroxylations (Table 2).

With regard to C-12b hydroxylation, the data could be best described using a sigmoidal equation (Figure S2H of the Supporting Information) as described previously for the wild-type enzyme.¹⁸ In general, the observed changes in catalytic efficiency (k_{cat}/S_{50}) were mostly caused by the rate of catalysis (k_{cat}) while the substrate concentration at which the reaction velocity was half the maximum (S_{50}) remained largely unchanged (Table 2). In comparison to that of the wild type, the efficiency of the $\beta 4$ – $\beta 5$ chimera in catalyzing C-12b hydroxylation was decreased to 1%. To pinpoint the associated secondary structure regions more precisely, the $\beta 4$ – $\beta 5$ region (Figure 1A) was divided into two halves. The exchange of the $\beta 4$ region (Table 1) into the JadH counterpart alone had no apparent effect on PgaE function, and the mutant behaved like the native enzyme. In contrast, the substitution of $\beta 5$ (Table 1) resulted in a corresponding decrease in C-12b hydroxylase activity as observed for the $\beta 4$ – $\beta 5$ region, confirming that the functional effects were confined to this C-terminal β -strand. Subsequent comparison of PgaE and JadH sequences within this region (Table 1) inferred that the effect could be caused by the steric effects imposed by I79 versus F90 in combination with P78 versus Q89, respectively. Accordingly, the P78Q/I79F double substitution resulted in a decrease in the efficiency of the enzyme to 8%. The equivalent single substitutions further revealed that the decrease in C-12b hydroxylase activity was mainly due to the I79F change, which showed a decrease in k_{cat}/S_{50} to 14%. Surprisingly, while the P78Q/I79F double substitution had a slight additional decreasing effect on C-12b hydroxylation activity, exchange of P78Q alone had an opposite impact and resulted in an ~2.5-fold increase in catalytic efficiency.

To estimate the effect of the amino acid substitutions on substrate inhibition in C-12 hydroxylation, the kinetic data were fit to various models, which indicated the presence of a minimum of two prejadomycin binding sites (text of the Supporting Information). However, the data allowed considerable flexibility in parameter values because of the insensitivity of the spectrophotometric assay, which led us to consider three models for constraining the fit parameters. Importantly, all of the methods yielded similar results (Table 2 and Figure S5 of the Supporting Information) and indicated that substrate inhibition was significantly alleviated (2–4-fold) in the $\beta 4$ – $\beta 5$, $\beta 5$, and I79F variants, but the data could not differentiate whether this was due to changes in (i) the affinity (K_M) for the substrate, (ii) the ratio of activities of the bisubstrate and monosubstrate ($V_{\text{ES2}}/V_{\text{ES}}$) complexes, or (iii) the ratio of dissociation constants of the bisubstrate and monosubstrate ($K_{\text{ES2}}/K_{\text{ES}}$) complexes. In the other variants, the apparent relaxation of substrate inhibition could be attributed to an ~1.5-fold elevated K_M (or K_{ES}) in P78Q and $\beta 4$, while the P78Q/I79F double mutant demonstrated kinetic behavior indistinguishable from that of the wild-type enzyme in terms of C-12 hydroxylation (Table 2).

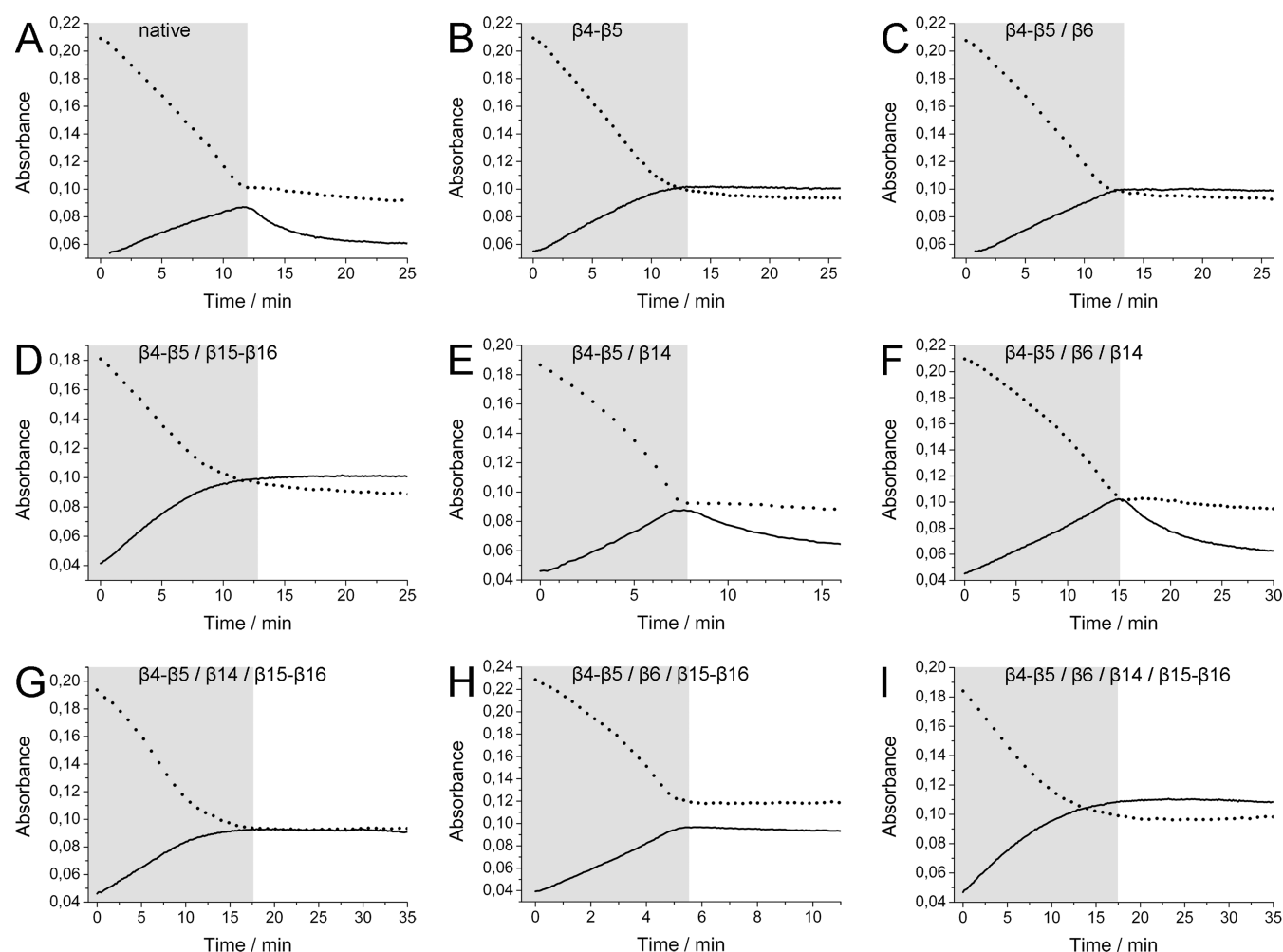


Figure 3. Spectrophotometric comparison of the two activities of chimeric PgaE enzymes using prejadomycin as a substrate. The consumption of the initial substrate prejadomycin can be followed as a decrease in the magnitude of the signal at 406 nm (···). The production and subsequent consumption of 12-hydroxyprejadomycin can be monitored as an increase and a decrease in absorbance at 510 nm (—), respectively.^{13,18} The two reactions occur in separate phases¹⁸ that are indicated by background color: (A) native PgaE, (B) the $\beta 4$ – $\beta 5$ single chimera, (C) the $\beta 4$ – $\beta 5/\beta 6$ double chimera, (D) the $\beta 4$ – $\beta 5/\beta 15$ – $\beta 16$ double chimera, (E) the $\beta 4$ – $\beta 5/\beta 14$ double chimera, (F) the $\beta 4$ – $\beta 5/\beta 6/\beta 14$ triple chimera, (G) the $\beta 4$ – $\beta 5/\beta 14/\beta 15$ – $\beta 16$ triple chimera, (H) the $\beta 4$ – $\beta 5/\beta 6/\beta 15$ – $\beta 16$ triple chimera, and (I) the $\beta 4$ – $\beta 5/\beta 6/\beta 14/\beta 15$ – $\beta 16$ quadruple chimera.

Table 2. Kinetic Parameters Determined for Native PgaE and the $\beta 4$ – $\beta 5$, $\beta 4$, $\beta 5$, P78Q/I79F, P78Q, I79F, and H73A Variants in Relation to C-12 Hydroxylation and C-12b Hydroxylation^a

PgaE variant	C-12 hydroxylation			C-12b hydroxylation		
	K_M	V_{ES2}/V_{ES}	K_{ES2}/K_{ES}	k_{cat} (s ^{−1})	S_{50} (μM)	k_{cat}/S_{50} (M ^{−1} s ^{−1})
native	3.14 ± 0.20	0.146 ± 0.010	2.21 ± 0.30	5.5 ± 0.2	18.6 ± 1.9	2.99 × 10 ⁵
$\beta 4$ – $\beta 5$	9.61 ± 0.31	0.254 ± 0.015	7.65 ± 0.53	0.124 ± 0.008	40.2 ± 5.7	3.10 × 10 ³
$\beta 4$	6.68 ± 0.38	0.115 ± 0.008	2.40 ± 0.30	5.3 ± 0.4	11.7 ± 2.9	4.54 × 10 ⁵
$\beta 5$	12.2 ± 0.4	0.322 ± 0.014	10.5 ± 0.6	0.28 ± 0.03	55.0 ± 9.3	5.07 × 10 ³
P78Q/I79F	3.95 ± 0.31	0.0977 ± 0.0054	2.95 ± 0.38	0.77 ± 0.05	33.0 ± 4.4	2.34 × 10 ⁴
P78Q	6.92 ± 0.29	0.158 ± 0.007	2.08 ± 0.21	24.0 ± 2.0	30.9 ± 5.0	7.76 × 10 ⁵
I79F	11.0 ± 0.3	0.273 ± 0.010	8.04 ± 0.49	1.23 ± 0.05	30.2 ± 3.3	4.09 × 10 ⁴
	k_{cat} (s ^{−1})	K_M (μM)	k_{cat}/K_M (M ^{−1} s ^{−1})			
H73A	1.8 ± 0.04	19.7 ± 0.9	9.06 × 10 ⁴			

^aSee the Supporting Information for details regarding the determination of substrate inhibition constants (K_M , V_{ES2}/V_{ES} , and K_{ES2}/K_{ES}) for C-12 hydroxylation (text and Figure S5 of the Supporting Information) and k_{cat} and S_{50} for C-12b hydroxylation (Figure S2 of the Supporting Information).

The Conserved H73 Is Important for C-12b Hydroxylation. In addition to the nonconserved residues between PgaE and JadH, the role of the invariant H73 was re-evaluated in light of the current understanding of PgaE.¹⁸ The residue is located in

$\beta 4$ adjacent to P78 and I79 in the immediate vicinity of the substrate binding site (Figure 1B) and is conserved in all known angucyclinone hydroxylases (Figure S3 of the Supporting Information). In the past, it has been shown that the residue is

not required for C-12 hydroxylation,²² but at the time of the investigation, the secondary activity of PgaE had not been discovered. Indeed, the H73A substitution did not prevent the conversion of prejadomycin but completely inhibited the C-12b hydroxylation step, resulting in the quantitative accumulation of the reaction intermediate. Importantly, the mutant no longer showed any signs of substrate inhibition in the C-12 hydroxylation reaction, and the reactions conformed to classical Michaelis–Menten saturation kinetics (Table 2 and text of the Supporting Information).

The Loss of C-12b Hydroxylation Activity of PgaE P78Q/I79F Cannot Be Discerned from the Structure. To evaluate the effect of the changes made to the $\beta 5$ region, the structure of the P78Q/I79F double mutant was determined to 2.4 Å resolution by protein crystallography. The protein crystallized in the open conformation, and in general, the quality of the electron density map (Figure S6 of the Supporting Information) and refinement statistics (Table S2 of the Supporting Information) were in agreement with the obtained resolution. However, in a manner similar to that of native PgaE,²² poor or no density was visible for segments of the middle domain. The overall structure of the mutant was highly similar to that of the native enzyme with a root-mean-square deviation of 0.3 Å. In essence, the structure confirmed that the bulkier side chain of I79F did not significantly alter the hydrophobic packing interactions against I357 residing in helix $\alpha 8$ and A363 and L366 in helix $\alpha 9$, and that the more flexible backbone of residue P78Q did not alter the main chain conformation of the $\beta 4$ – $\beta 5$ sheet region (Figure 1B). Finally, the structure verified that the side chains of the mutated residues reside close to the dimer interface and in effect point away from the active site cavity (Figure 1C).

DISCUSSION

One of the central concepts in enzyme molecular evolution is functional promiscuity,^{38,39} the existence of hidden, context-dependent, secondary catalytic activities, which have the potential to evolve into new functionalities under different selective conditions. Of the several evolutionary models around this premise,⁷ the escape from adaptive conflict (EAC) focuses specifically on the development of promiscuous enzymes into bifunctional catalytic entities prior to possible gene duplication and specialization.^{40,41} The model explains the concomitant evolution of new functions and conservation of old functions in a single enzyme and applies well to rapidly evolving secondary metabolic pathways such as those in angucycline biosynthesis (Scheme 1).¹³ In the case of NADPH-dependent flavoprotein angucycline hydroxylases, certain lines of evidence suggest that the common ancestral form was a monooxygenase responsible for C-12 hydroxylation, which nonetheless harbored promiscuous C-12b hydroxylation and C-4a/C-12b dehydration activities. This is supported by the residual C-12b hydroxylase activity by JadH, which could be exclusively detected *in vitro* when 12-hydroxypredomycin was used as a substrate,¹³ thus indicating that the ancestral activity has not been completely lost in the course of enzyme evolution. On the other hand, while we have not been able to observe the C-4a/C-12b dehydration activity of JadH with enzymes involved in benz[*a*]anthracene biosynthesis, indirect evidence suggests that these enzymes are responsible for a similar C-4a/C-12b dehydration reaction during landomycin biosynthesis.¹³ The evolution of these promiscuous functions into true secondary C-12b hydroxylation and C-4a/C-12b dehydration activities represents the branching point in the biosynthesis of many important angucycline metabolites

(Scheme 1).^{12,13,18,19} In general, the contemporary evolutionary models consider bifunctional enzymes such as PgaE and JadH merely as an intermediate step in the process toward specialized monofunctional enzymes,⁷ but the extent to which such optimization takes place in secondary metabolism remains unclear.

One aim of this study was to determine the structural regions related to the diversification of the functions of JadH and PgaE. Our approach was to first replace relatively large regions (up to 13 amino acid residues at a time) in PgaE with the corresponding residues found in JadH and then to pinpoint the individual amino acid residues or regions responsible for the functional differences. The mutagenesis results clearly demonstrated that the native C-12b hydroxylase activity of PgaE was dependent on strand $\beta 5$ at the far end of the active site cleft. Replacing the strand with the JadH counterpart resulted in a decrease of activity to 2%, which corresponds to the residual activity found in JadH,¹³ while the C-12 hydroxylase activity was mostly unaffected. Residue I79 within this region was shown to play an important role in the reaction as the I79F substitution resulted in a significant decrease in catalytic efficiency, and the additional P78Q substitution slightly enhanced the effect. Therefore, we can conclude that two point mutations to PgaE (ccgac to cagtc) were sufficient for the loss of C-12b hydroxylase activity. From the evolutionary viewpoint, the mutations at these sites may represent the pivotal turning point that allowed the existing promiscuous C-12b hydroxylase activity to evolve into the second catalytic function of PgaE. The importance of this region is also supported by the multiple-sequence analysis, which demonstrates that the related C-12 and C-12b hydroxylases CabE, LanE, and UrdE also have a proline and a neutral nonpolar residue at the positions corresponding to the glutamine and phenylalanine in JadH and AlpG, respectively (Figure S3 of the Supporting Information). However, the sequence conservation does not extend to the more distantly related GilOI (Figure 2),²⁰ which appears to have gone through numerous additional changes in the entire $\beta 4$ – $\beta 5$ region (Figure S3 of the Supporting Information).

In addition to the minimal evolutionary distance described above, the chimeragenesis approach clearly demonstrated that there may be several alternative routes leading to the same end result. First, replacing the $\beta 4$ – $\beta 5$ region (seven amino acid substitutions) in PgaE impaired the native C-12b hydroxylase activity. Further modification of the enzyme toward JadH, however, restored the native activity in the $\beta 4$ – $\beta 5$ / $\beta 6$ / $\beta 14$ triple chimera (12 amino acid substitutions). Remarkably, the change of another six additional residues resulted, again, in the loss of C-12b hydroxylase function in the $\beta 4$ – $\beta 5$ / $\beta 6$ / $\beta 14$ / $\beta 15$ – $\beta 16$ quadruple chimera (18 amino acid substitutions). The results indicate that the PgaE active site is surprisingly malleable and that the enzymatic activity is determined by the cumulative effects of minor differences in multiple regions. Despite the extensive engineering of the active site cavity of PgaE, even the quadruple chimera did not gain the C-4a/C-12b dehydration activity of JadH. This suggests that the activity may depend on even more distal regions of the proteins, because practically all invariant amino acids lining the active site have been exchanged in the quadruple chimera (Figure 1A).

The flavoenzyme PgaE contains several unusual features, which include bifunctionality, the temporal separation of two reactions, and substrate inhibition in the case of the first, but not the second, reaction. In this study, we have shown a correlation between substrate inhibition and C-12b hydroxylation activity; enzyme variants with reduced C-12b hydroxylation activity also

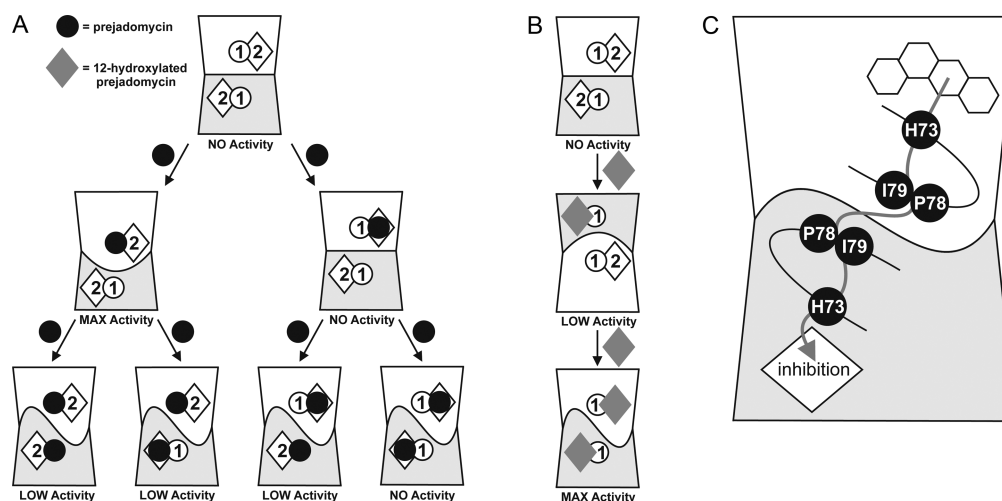


Figure 4. Model explaining the function of PgaE and the effects caused by mutagenesis of the $\beta 4$ – $\beta 5$ region. The two monomers of the PgaE dimer are colored white and gray, while the two overlapping binding sites for C-12 and C-12b hydroxylation are depicted as 1 in a circle and 2 in a diamond, respectively. Allosteric interactions are represented by the shape of the line between the two monomers. (A) In C-12 hydroxylation, the substrate prejadomycin (black circle) may bind to the sites for C-12 and C-12b hydroxylations leading to catalysis and substrate inhibition, respectively. Binding of the first molecule of prejadomycin induces an allosteric effect, which lowers the enzymatic activity of the bisubstrate complex. (B) In C-12b hydroxylation after depletion of prejadomycin, the substrate (gray diamond) may bind only to the orientation for the second C-12b hydroxylation and the enzymatic activity is mainly derived from the bisubstrate complex. (C) The allosteric substrate inhibition in C-12 hydroxylation is conveyed via H73, P78, and I79 across the dimer interface to the other subunit.

displayed relaxed substrate inhibition in the C-12 hydroxylation reaction (Table 2). A model that could best explain all of the observed characteristics of PgaE is presented in Figure 4. It is likely that the enzyme hosts two overlapping binding modes, one each for C-12 and C-12b hydroxylations. Binding of prejadomycin to the orientation for C-12 hydroxylation leads to catalysis, while binding in the other orientation is non-productive (Figure 4A). In addition, the kinetic data revealed the presence of a second binding site for prejadomycin, where binding inhibits the catalytic cycle in a noncompetitive manner. Because the size of the active site cavity appears to be too small to accommodate two nonoverlapping binding sites and we identified mutations residing at the dimerization interface that affected the pattern of substrate inhibition, it appears possible that the inhibition by excess prejadomycin is due to allosteric interactions between the two active sites within the PgaE dimer. In other words, the binding of two substrate molecules at high prejadomycin concentrations to both monomers leads to decreased catalytic efficiency, which is observed as substrate inhibition (Figure 4A). The stringent temporal separation of the C-12 and C-12b hydroxylation events¹⁸ could be explained by the model if the binding of prejadomycin to either one of the monomers would prevent the productive association of the substrate for the second reaction, 12-hydroxy-prejadomycin. The inhibition in this case would be both competitive (binding to the same monomer) and allosteric (binding on different monomers). After depletion of prejadomycin, the substrate for the second reaction may bind only in the orientation for C-12b hydroxylation, and therefore, no substrate inhibition is observed (Figure 4B). Furthermore, the kinetic data for the second reaction could be best described with a sigmoidal relationship (Figure S2H of the Supporting Information),¹⁸ which implies that substrate binding is cooperative and the activity is largely derived from the bisubstrate complex, which may therefore additionally contribute to the temporal separation of the C-12 and C-12b reactions. However, it should be noted that verification of the model will require analysis of pre-steady-

state kinetic data in the future because of the limitations imposed by relying solely on steady-state kinetics. The model presented here promotes the notion that in the case of PgaE substrate inhibition is not essential for the function or regulation of the enzymatic activity, as has been suggested for many other proteins,⁴² but rather a consequence of the ability of the protein to catalyze C-12b hydroxylation.

The two successive PgaE-catalyzed hydroxylation reactions are expected to proceed in a mechanistically equivalent manner, involving the typical NADPH- and O₂-dependent FAD redox cycle coupled to the transition between open and closed conformations of the enzyme.^{18,43} The critical difference between the two reactions is apparently the orientation of the bound substrate, and its alignment with the reactive FAD 4a-hydroperoxide intermediate that determines the hydroxylation regioselectivity between C-12 and C-12b. Despite the fact that PgaE crystallizes in the open conformation, it seems clear that strand $\beta 5$ or residues P78 and I79 are not in the immediate vicinity of the FAD or in direct contact with the substrate. The P78Q and I79F substitutions are unlikely to have any mechanistic role in catalysis but may rather be related to changes in conformational movement during the transition into the closed tertiary structure upon ligand binding. The observed effects on C-12b hydroxylation by these variants may therefore be due to indirect interactions, possibly via the invariant residue H73, which affects the topology of the binding site and either allows or disallows the substrate to align correctly for the second hydroxylation reaction. The P78Q/I79F double variant appears to be exceptional because it is the only mutant in which the connection between C-12b hydroxylation and substrate inhibition does not exist; the enzyme displays 10-fold reduced C-12b hydroxylation efficiency while harboring levels of substrate inhibition similar to that of the wild type (Table 2). In contrast, the kinetic data for the H73A variant may be fit with a simple kinetic model (Figure S5D of the Supporting Information), which contains only one independent binding site that does not require cooperativity between the two

monomers of PgaE. Furthermore, according to the data, the substrate inhibitory site is no longer present, and the product and the substrate compete for the same site with the same affinity. The mutagenesis experiments therefore reveal the importance of H73 for the allosteric network and indicate that I79 and possibly P78 are important in communicating the information to the other enzyme subunit (Figure 4C).

In closing, it may be noteworthy to contemplate the benefits of the modified four-primer chimeragenesis approach introduced here. Our results clearly show that catalytic properties of PgaE are strongly affected by residues situated at a relatively large distance from the putative substrate binding site, that could have been very difficult to identify with traditional mutagenesis relying on single or double mutations near the catalytic core region. The work demonstrates how swapping of relatively long polypeptide stretches between homologous enzymes allows efficient screening of catalytically significant regions. This narrows the range of potentially interesting areas and can then be used to further pinpoint the exact individual residues of specific interest.

■ ASSOCIATED CONTENT

■ Supporting Information

Details of analysis of the conversion kinetics of C-12 and C-12b hydroxylations, SDS-PAGE analysis of the PgaE variants, structure-based multiple-sequence alignment of angucycline hydroxylases, crystallographic data collection and refinement statistics, oligonucleotide primers utilized in the study, and the electron density map of the $\beta 4$ – $\beta 5$ region of PgaE P78Q/I79F. This material is available free of charge via the Internet at <http://pubs.acs.org>.

Accession Codes

The atomic coordinates have been deposited in the Protein Data Bank as entry 4ICY.

■ AUTHOR INFORMATION

Corresponding Author

*Department of Biochemistry and Food Chemistry, University of Turku, FIN-20014 Turku, Finland. Phone: +35823336846. Fax: +35822317666. E-mail: mikko.mk@gmail.com.

Funding

This study was supported by the Academy of Finland (Grants 130581 to G.A.B., 121688 to J.N., 127844 to P.M., and 136060 to M.M.-K.), the National Natural Science Foundation of China (Grant 31130001 to K.Y.), and the National Doctoral Programme in Informational and Structural Biology.

Notes

The authors declare no competing financial interest.

■ ACKNOWLEDGMENTS

We thank Keshav Thapa for help with the docking experiments. We gratefully acknowledge access to synchrotron radiation at the European Synchrotron Radiation Facility, Grenoble, France.

■ REFERENCES

- (1) Newman, D. J., and Cragg, G. M. (2012) Natural products as sources of new drugs over the 30 years from 1981 to 2010. *J. Nat. Prod.* 75, 311–335.
- (2) Nett, M., Ikeda, H., and Moore, B. S. (2009) Genomic basis for natural product biosynthetic diversity in the actinomycetes. *Nat. Prod. Rep.* 26, 1362–1384.
- (3) Fu, D. H., Jiang, W., Zheng, J. T., Zhao, G. Y., Li, Y., Yi, H., Li, Z. R., Jiang, J. D., Yang, K. Q., Wang, Y., and Si, S. Y. (2008) Jadomycin B, an

Aurora-B kinase inhibitor discovered through virtual screening. *Mol. Cancer Ther.* 7, 2386–2393.

(4) Hasinoff, B. B., Wu, X., Yalowich, J. C., Goodfellow, V., Laufer, R. S., Adedayo, O., and Dmitrienko, G. I. (2006) Kinamycins A and C, bacterial metabolites that contain an unusual diazo group, as potential new anticancer agents: Antiproliferative and cell cycle effects. *Anticancer Drugs* 17, 825–837.

(5) McGee, L. R., and Misra, R. (1990) Gilvocarcin photobiology: Isolation and characterization of the DNA photoadduct. *J. Am. Chem. Soc.* 112, 2386–2389.

(6) Korynevska, A., Heffeter, P., Matselyukh, B., Elbling, L., Micksche, M., Stoika, R., and Berger, W. (2007) Mechanisms underlying the anticancer activities of the angucycline landomycin E. *Biochem. Pharmacol.* 74, 1713–1726.

(7) Conant, G. C., and Wolfe, K. H. (2008) Turning a hobby into a job: How duplicated genes find a new job. *Nat. Rev. Genet.* 9, 938–950.

(8) Jansson, A., Koskiniemi, H., Erola, A., Wang, J., Mäntsälä, P., Schneider, G., and Niemi, J. (2005) Aclacinomycin 10-hydroxylase is a novel substrate-assisted hydroxylase requiring S-adenosyl-L-methionine as cofactor. *J. Biol. Chem.* 280, 3636–3644.

(9) Siitonen, V., Blauenburg, B., Kallio, P., Mäntsälä, P., and Metsä-Ketelä, M. (2012) Discovery of a two-component monooxygenase SnoaW/SnoaL2 involved in nogalamycin biosynthesis. *Chem. Biol.* 19, 638–646.

(10) Beinker, P., Lohkamp, B., Peltonen, T., Niemi, J., Mäntsälä, P., and Schneider, G. (2006) Crystal structures of SnoaL2 and AclR: Two putative hydroxylases in the biosynthesis of aromatic polyketide antibiotics. *J. Mol. Biol.* 359, 728–740.

(11) Sultana, A., Kallio, P., Jansson, A., Wang, J. S., Niemi, J., Mäntsälä, P., and Schneider, G. (2004) Structure of the polyketide cyclase SnoaL reveals a novel mechanism for enzymatic aldol condensation. *EMBO J.* 23, 1911–1921.

(12) Chen, Y., Fan, K., He, Y., Xu, X., Peng, Y., Yu, T., Jia, C., and Yang, K. (2010) Characterization of JadH as an FAD- and NAD(P)H-dependent bifunctional hydroxylase/dehydrase in jadomycin biosynthesis. *ChemBioChem* 11, 1055–1060.

(13) Patrikainen, P., Kallio, P., Fan, K., Klika, K. D., Shaaban, K. A., Mäntsälä, P., Rohr, J., Yang, K., Niemi, J., and Metsä-Ketelä, M. (2012) Tailoring enzymes involved in the biosynthesis of angucyclines contain latent context-dependent catalytic activities. *Chem. Biol.* 19, 647–655.

(14) Kharel, M. K., Pahari, P., Shepherd, M. D., Tibrewal, N., Nybo, S. E., Shaaban, K. A., and Rohr, J. (2012) Angucyclines: Biosynthesis, mode-of-action, new natural products, and synthesis. *Nat. Prod. Rep.* 29, 264–325.

(15) Hertweck, C., Luzhetskyy, A., Rebets, Y., and Bechthold, A. (2007) Type II polyketide synthases: Gaining a deeper insight into enzymatic teamwork. *Nat. Prod. Rep.* 24, 162–190.

(16) Metsä-Ketelä, M., Palmu, K., Kunnari, T., Ylihonko, K., and Mäntsälä, P. (2003) Engineering anthracycline biosynthesis toward angucyclines. *Antimicrob. Agents Chemother.* 47, 1291–1296.

(17) Kharel, M. K., Pahari, P., Shaaban, K. A., Wang, G., Morris, C., and Rohr, J. (2012) Elucidation of post-PKS tailoring steps involved in landomycin biosynthesis. *Org. Biomol. Chem.* 10, 4256–4265.

(18) Kallio, P., Patrikainen, P., Suomela, J. P., Mäntsälä, P., Metsä-Ketelä, M., and Niemi, J. (2011) Flavoprotein hydroxylase PgaE catalyzes two consecutive oxygen-dependent tailoring reactions in angucycline biosynthesis. *Biochemistry* 50, 5535–5543.

(19) Pahari, P., Kharel, M. K., Shepherd, M. D., van Lanen, S. G., and Rohr, J. (2012) Enzymatic total synthesis of defucogilvogarcin M and its implications for gilvogarcin biosynthesis. *Angew. Chem., Int. Ed.* 51, 1216–1220.

(20) Palmu, K., Ishida, K., Mäntsälä, P., Hertweck, C., and Metsä-Ketelä, M. (2007) Artificial reconstruction of two cryptic angucycline antibiotic biosynthetic pathways. *ChemBioChem* 8, 1577–1584.

(21) Gould, S. J., Hong, S. T., and Carney, J. R. (1998) Cloning and heterologous expression of genes from the kinamycin biosynthetic pathway of *Streptomyces murayamaensis*. *J. Antibiot.* 51, 50–57.

(22) Koskiniemi, H., Metsä-Ketelä, M., Dobritsch, D., Kallio, P., Korhonen, H., Mäntsälä, P., Schneider, G., and Niemi, J. (2007) Crystal

structures of two aromatic hydroxylases involved in the early tailoring steps of angucycline biosynthesis. *J. Mol. Biol.* 372, 633–648.

(23) Wierenga, R. K., de Jong, R. J., Kalk, K. H., Hol, W. G., and Drenth, J. (1979) Crystal structure of p-hydroxybenzoate hydroxylase. *J. Mol. Biol.* 131, 55–73.

(24) Schreuder, H. A., Prick, P. A., Wierenga, R. K., Vriend, G., Wilson, K. S., Hol, W. G., and Drenth, J. (1989) Crystal structure of the p-hydroxybenzoate hydroxylase-substrate complex refined at 1.9 Å resolution. Analysis of the enzyme-substrate and enzyme-product complexes. *J. Mol. Biol.* 208, 679–696.

(25) Entsch, B., Cole, L. J., and Ballou, D. P. (2005) Protein dynamics and electrostatics in the function of p-hydroxybenzoate hydroxylase. *Arch. Biochem. Biophys.* 433, 297–311.

(26) Enroth, C., Neujahr, H., Schneider, G., and Lindqvist, Y. (1998) The crystal structure of phenol hydroxylase in complex with FAD and phenol provides evidence for a concerted conformational change in the enzyme and its cofactor during catalysis. *Structure* 6, 605–617.

(27) Ballou, D. P., Entsch, B., and Cole, L. J. (2005) Dynamics involved in catalysis by single-component and two-component flavin-dependent aromatic hydroxylases. *Biochem. Biophys. Res. Commun.* 338, 590–598.

(28) Ho, S. N., Hunt, H. D., Horton, R. M., Pullen, J. K., and Pease, L. R. (1989) Site-directed mutagenesis by overlap extension using the polymerase chain reaction. *Gene* 77, 51–59.

(29) Kallio, P., Sultana, A., Niemi, J., Mäntsälä, P., and Schneider, G. (2006) Crystal structure of the polyketide cyclase AklH with bound substrate and product analogue: Implications for catalytic mechanism and product stereoselectivity. *J. Mol. Biol.* 357, 210–220.

(30) Bradford, M. M. (1976) A rapid and sensitive method for the quantitation of microgram quantities of protein utilizing the principle of protein-dye binding. *Anal. Biochem.* 72, 248–254.

(31) Leslie, A. G. W., and Powell, H. R. (2007) in *Evolving Methods for Macromolecular Crystallography* (Read, R. J., and Sussman, J. L., Eds.) pp 41–51, Springer, Heidelberg, Germany.

(32) Collaborative Computational Project, Number 4 (1994) The CCP4 suite: Programs for protein crystallography. *Acta Crystallogr. D* 50, 760–763.

(33) Vagin, A., and Teplyakov, A. (1997) MOLREP: An automated program for molecular replacement. *J. Appl. Crystallogr.* 30, 1022–1025.

(34) Emsley, P., Lohkamp, B., Scott, W. G., and Cowtan, K. (2010) Features and development of Coot. *Acta Crystallogr. D* 66, 486–501.

(35) Murshudov, G. N., Vagin, A., and Dodson, E. J. (1997) Refinement of macromolecular structures by the maximum-likelihood method. *Acta Crystallogr. D* 53, 240–255.

(36) Chen, V. B., Arendall, W. B., III, Headd, J. J., Keedy, D. A., Immormino, R. M., Kapral, G. J., Murray, L. W., Richardson, J. S., and Richardson, D. C. (2010) MolProbity: All-atom structure validation for macromolecular crystallography. *Acta Crystallogr. D* 66, 12–21.

(37) Schüttelkopf, A. W., and van Aalten, D. M. (2004) PRODRG: A tool for high-throughput crystallography of protein-ligand complexes. *Acta Crystallogr. D* 60, 1355–1363.

(38) Copley, S. D. (2003) Enzymes with extra talents: Moonlighting functions and catalytic promiscuity. *Curr. Opin. Chem. Biol.* 7, 265–272.

(39) Khersonsky, O., and Tawfik, D. S. (2010) Enzyme promiscuity: A mechanistic and evolutionary perspective. *Annu. Rev. Biochem.* 79, 471–505.

(40) Des Marais, D. L., and Rausher, M. D. (2008) Escape from adaptive conflict after duplication in an anthocyanin pathway gene. *Nature* 454, 762–765.

(41) Sikosek, T., Chan, H. S., and Bornberg-Bauer, E. (2012) Escape from Adaptive Conflict follows from weak functional trade-offs and mutational robustness. *Proc. Natl. Acad. Sci. U.S.A.* 109, 14888–14893.

(42) Reed, M. C., Lieb, A., and Nijhout, H. F. (2010) The biological significance of substrate inhibition: A mechanism with diverse functions. *BioEssays* 32, 422–429.

(43) van Berkel, W. J., Kamerbeek, N. M., and Fraaije, M. W. (2006) Flavoprotein monooxygenases, a diverse class of oxidative biocatalysts. *J. Biotechnol.* 124, 670–689.